Nonhematopoietic antigen blocks memory programming of alloreactive CD8+ T cells and drives their eventual exhaustion in mouse models of bone marrow transplantation

Barry Flutter,[1] Noha Edwards,[1] Farnaz Fallah-Arani,[1] Stephen Henderson,[2] Jian-Guo Chai,[3] Shivajanani Sivakumaran,[1] Sara Ghorashian,[1] Clare L. Bennett,[1] Gordon J. Freeman,[4] Megan Sykes,[5] and Ronjon Chakraverty[1]

[1]Transplantation Immunology Group, Department of Haematology, and [2]Cancer Research UK Viral Oncology Group, University College London, London, United Kingdom. [3]Department of Immunology, Faculty of Medicine, Imperial College London, London, United Kingdom. [4]Department of Medical Oncology, Dana-Farber Cancer Institute, Harvard Medical School, Boston, Massachusetts, USA. [5]Columbia Center for Translational Immunology, Columbia University Medical Center, New York, New York, USA.

Allogeneic blood or BM transplantation (BMT) is the most commonly applied form of adoptive cellular therapy for cancer. In this context, the ability of donor T cells to respond to recipient antigens is coopted to generate graft-versus-tumor (GVT) responses. The major reason for treatment failure is tumor recurrence, which is linked to the eventual loss of functional, host-specific CTLs. In this study, we have explored the role of recipient antigen expression by nonhematopoietic cells in the failure to sustain effective CTL immunity. Using clinically relevant models, we found that nonhematopoietic antigen severely disrupts the formation of donor CD8+ T cell memory at 2 distinct levels that operate in the early and late phases of the response. First, initial and direct encounters between donor CD8+ T cells and nonhematopoietic cells blocked the programming of memory precursors essential for establishing recall immunity. Second, surviving CD8+ T cells became functionally exhausted with heightened expression of the coinhibitory receptor programmed death-1 (PD-1). These 2 factors acted together to induce even more profound failure in long-term immunosurveillance. Crucially, the functions of exhausted CD8+ T cells could be partially restored by late in vivo blockade of the interaction between PD-1 and its ligand, PD-L1, without induction of graft-versus-host disease, suggestive of a potential clinical strategy to prevent or treat relapse following allogeneic BMT.

Introduction

Allogeneic blood or BM transplantation (BMT) represents the most commonly applied form of adoptive cellular therapy for cancer. This treatment exploits donor T cell alloreactivity to generate a graft-versus-tumor (GVT) effect (1, 2). Since the antigens targeted in this response may have ubiquitous expression, one major limitation of this approach is the risk of immune-mediated injury to peripheral tissues, in the form of graft-versus-host disease (GVHD). Transfer of donor T cells immediately following recipient conditioning heightens this risk as a result of the proinflammatory milieu (3–5). In this context, alloantigen-specific memory T cells with self-renewal potential may emerge early in the response and continually replenish the pool of effectors, thus perpetuating host injury (6).

Both experimental and clinical data have demonstrated that delaying transfer of donor T cells following conditioning can deliver effective GVT responses while limiting the risk of GVHD (1, 7–9). The approach of delayed donor leukocyte infusion (DLI) is widely applied in the clinic, particularly following nonmyeloablative transplantation protocols (10). In this context, host hematopoietic elements that persist after initial transplantation can prime incoming donor T cells, leading to an antihost response that induces conversion to full donor chimerism (in which remaining

host hematopoietic cells are rejected) and accompanying antitumor effects (11–14). Unfortunately, the most common reason for treatment failure with this strategy is relapse (1). Transfer of donor T cells to a noninflammatory environment may partially compromise the capacity of such cells to acquire a full repertoire of effector functions (7, 15, 16). Furthermore, initial alloreactive responses may be poorly sustained with the eventual loss of functional CTL (17, 18). The mechanisms underlying this failure to provide effective and durable immunosurveillance are not known.

An important distinction between the GVT response and T cell responses to acute infections is that, in the former situation, antigen persists following the initial primary response. In this respect, the immune response occurs under circumstances similar to those that occur in chronic infections or solid cancers, where antigen is not cleared and functional antigen-specific T cells are also eventually lost (reviewed in refs. 19, 20). In these settings, both early fate decisions (survival and memory precursor formation) and late fitness of antigen-specific CD8+ populations can be compromised. At its most extreme, CD8+ populations with specificity for immunodominant epitopes may be deleted entirely from the repertoire (21). Alternatively, persistence of viral antigens or tumor-associated self antigens may instead drive exhaustion, in which surviving cells become subject to strong coinhibitory signals in the host and progressively lose effector function (22–24).

Our current understanding of early fate determination and late fitness of CD8+ T cells necessarily invokes the role of BM-derived

professional APCs. Professional APCs are highly proficient in integrating signals from the host environment (e.g., inflammation) or other interacting cells (e.g., CD4+ helper cells) that are critical to the initial programming of CD8+ memory differentiation (25). However, the recent finding that memory precursors can arise from cytolytic effector cells (26–28) suggests that it is also important to consider how early interactions with target cells might dictate the eventual fate of CD8+ cells. Similarly, although persistent antigen presentation by hematopoietic APCs has been shown to be sufficient for driving exhaustion (29), whether this mode of presentation is required is not known. In this regard, recent studies have observed compartmentalization of exhausted CD8+ cells within the livers of patients with chronic viral hepatitis (30) or within solid tumors (31). Expression of coinhibitory molecules by nonhematopoietic cells within these environments could contribute to downregulation of effector T cell functions in the long term (32). These observations suggest that it is important to consider the role of antigen expression by nonhematopoietic tissues in shaping not only initial imprinting of CD8+ cell memory fate, but also long-term fitness in the face of persistent antigen.

This issue is of particular relevance to the GVT response following delayed DLI. In this case, incoming CD8+ T cells interact with a noninflamed host environment in which antigen is expressed both by nonhematopoietic cells and by residual host hematopoietic cells. Thereafter, host antigen is cleared from the hematopoietic system by the ensuing donor T cell response, but continues to be expressed by cells within the nonhematopoietic compartment (for example, in peripheral tissues, the vasculature or the stroma of lymphoid organs). Although cross-presentation of host antigens by donor hematopoietic APCs may occur, this process is likely to be less efficient in the absence of inflammation (33), or less important when responses are directed at MHC alloantigens (11, 13, 16). It therefore follows that any influence of the nonhematopoietic compartment upon the fate of alloreactive T cell populations might in fact depend upon direct interactions with nonhematopoietic cells rather than professional APCs. To address this issue, we examined the functions of donor T cells in murine models of BMT and delayed DLI. By manipulating the presence of antigen within the periphery, we found that nonhematopoietic tissues drive CD8+ dysfunction at 2 distinct levels. First, the nonhematopoietic compartment critically regulated early fate decisions and blocked imprinting of CD8+ memory differentiation. Second, direct presentation of antigen by nonhematopoietic cells led to a progressive diminution in donor CD8+ cell function as a consequence of exhaustion, further contributing to the deficit in long-term immunosurveillance. These findings have important implications for immunotherapeutic strategies designed to preserve the integrity of T cell function over the long term.

Results

Eventual loss of CD8+ cell alloreactivity following delayed transfer of donor T cells to allogeneic chimeras. To determine the fate of donor CD8+ T cells upon transfer to allogeneic chimeras, we first used a murine model representative of nonmyeloablative transplantation and delayed DLI (3, 15). In selection of the appropriate model to explore the interaction of donor CD8+ cells with host nonhematopoietic cells, it was desirable to use an experimental system in which cross-presentation of host antigens by donor hematopoietic cells would not contribute significantly to the donor CD8+ response. In this regard, we have previously reported that the donor CD8+ cell response following delayed

DLI to fully MHC-mismatched allogeneic chimeras does not involve significant cross-presentation of host antigens (11, 13).

We confirmed that this requirement was also met in a model involving a partial MHC mismatch, whereby C57BL/6 (B6) CD45.1+ donor T cells were transferred to established allogeneic chimeras generated by reconstitution of lethally irradiated B6 (H-2b) × DBA/2 (H-2d) [BDF1, H-2bxd] mice with a mix of T cell–depleted host (BDF1) and donor (B6) BM (3, 15). The resulting stable chimeras (referred to herein as [B6+BDF1→BDF1]) had between 40% and 60% host hematopoiesis. Transfer of donor T cells at 8–12 weeks following reconstitution and following recovery from lymphopenia led to expansion of donor T cells (Figure 1, A and B, and Supplemental Figure 1; supplemental material available online with this article; doi:10.1172/JCI41446DS1) and eradication of host hematopoietic elements, but not to GVHD (3). Very similar findings were observed in the same strain combination using nonmyeloablative conditioning regimens based upon clinical protocols (ref. 3 and our unpublished observations). In the absence of host BM-derived cells, cross-priming of an antihost T cell response did not occur, as shown by a failure to observe CD8+ proliferation in established [B6→BDF1] chimeras (Supplemental Figure 1).

Following initial transfer, the number of CD45.1+ CD8+ cells increased rapidly, peaking at day 12 and contracting thereafter (Figure 1B). However, 60 days following transfer, there were still substantial numbers of CD45.1+ CD8+ cells in recipient secondary lymphoid organs (approximately 5%–10% of peak values), which suggests that the T cell repertoire still contained alloantigen-primed CD8+ cells. To determine the capacity of donor CD8+ cells to mediate antihost reactivity over time, we performed in vivo cytotoxicity assays involving cotransfer of F1 host and parental donor target B cells differentially labeled with CFSE (Figure 1C). This assay is largely representative of donor CTL activity, since alloreactive NK cells do not play a major role in rejection of F1 targets (34). Although robust cytotoxicity against host targets was evident at day 12–14 following T cell transfer, specific cytotoxicity was significantly reduced by day 60. At this later time point, detectable CTL function could not be recovered following either in vitro stimulation with host APCs or i.p. vaccination with host-type LPS-activated dendritic cells (data not shown). Compared with day 12, CD45.1+ CD8+ cells at day 60 proliferated less to alloantigen (Figure 1D) and demonstrated a decline in their capacity to generate IFN-γ (Figure 1E), albeit from a low initial level in the latter case (15). These data demonstrate a profound failure of host antigen–reactive CD8+ populations to sustain their functions in the long term.

Antigen expression by nonhematopoietic tissues disrupts memory function and homeostasis. We hypothesized that persistent antigen expression by nonhematopoietic cells was responsible for impairing memory formation and/or homeostasis. In order to test this concept, we wanted to compare the fate of alloreactive CD8+ cells in mice in which nonhematopoietic tissue antigen (nhTA) was either present or absent (nhTA+ or nhTA–, respectively) following the initial phase of the response. Thus, 3 × 10^7 B6 CD45.1+ splenocytes (SCs) were transferred to established [B6+BDF1→BDF1] (i.e., nhTA+) or [B6+BDF1→B6] (i.e., nhTA–) chimeras (Figure 2A). In both groups, BDF1 BM-derived cells were available to prime the initial response leading to the eradication of BDF1 hematopoietic elements, but only in nhTA+ chimeras did antigen remain. In each set of chimeras, the proportion of BDF1 hematopoietic cells was very similar at the time of transfer (Supplemental Figure 2). By day 28, BDF1 hematopoietic elements had been cleared
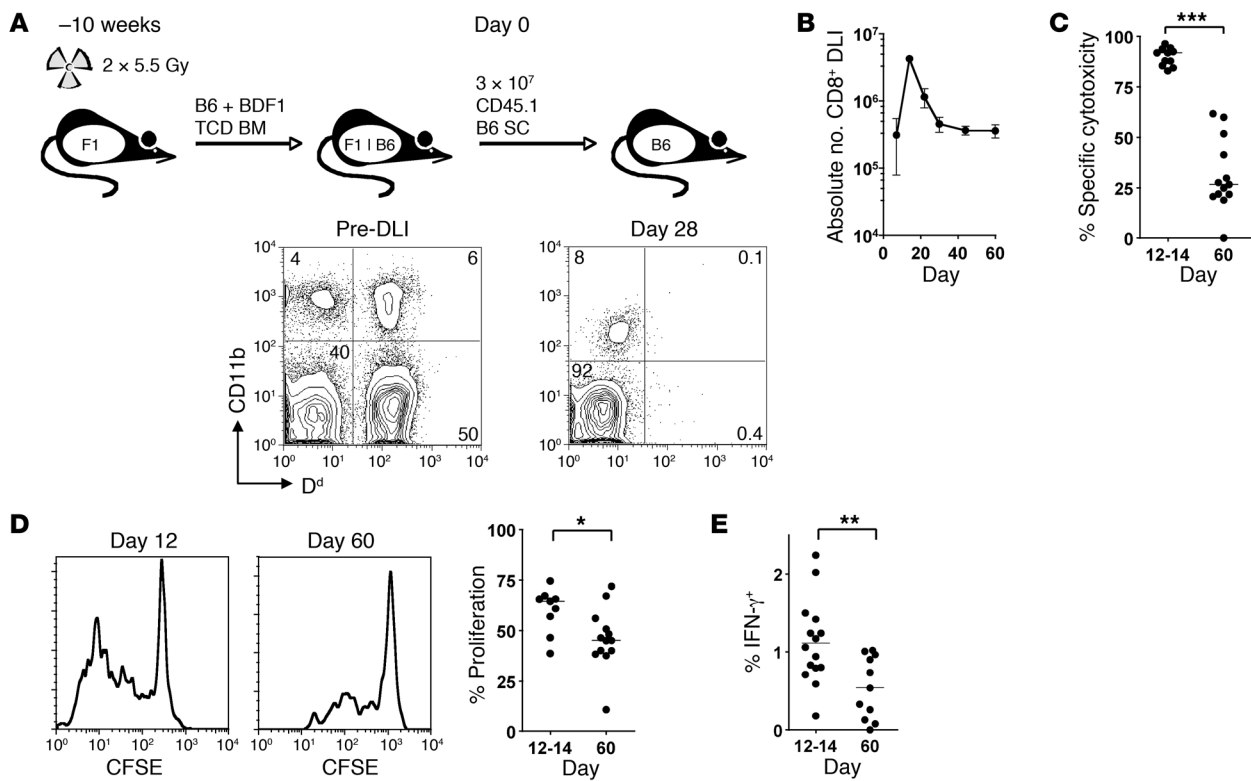
Figure 1

CD8^{+} T cells transferred to established mixed chimeras show transient cytotoxicity followed by loss of effector function. (**A**) Allogeneic chimeras were generated by lethal irradiation of recipient BDF1 (F1) mice followed by reconstitution with T cell–depleted (TCD) B6 and BDF1 BM. 10 weeks later, 3×10^7 CD45.1[+] B6 SCs were transferred to established chimeras. A representative example of blood chimerism of mice before and 28 days after DLI is shown using D[d] as a marker of BDF1-derived cells. (**B**) Absolute number of CD45.1^{+} CD8^{+} T cells recovered from the spleen at various times following DLI (*n* = 3 per group per time point). (**C**) A 1:1 mix of CFSE^{hi} and CFSE^{lo} labeled B6 and BDF1 B cells, respectively, were injected intravenously into mice 12 or 60 days after DLI. In vivo cytotoxicity was measured by the disappearance of injected BDF1 B cells relative to B6 B cells after 15 hours. (**D**) SCs isolated from recipients at 12 or 60 days were CFSE labeled and stimulated for 5 days with irradiated BDF1 SCs. Shown are representative histograms of proliferation of transferred CD8^{+} T cells and summary data of the percentage of cells that had divided 2 or more times. (**E**) SCs were restimulated overnight with irradiated BDF1 SCs, and production of IFN-γ by donor CD8^{+} T cells was measured by intracellular cytokine staining and flow cytometry. Scatter plot indicates the percentage of CD45.1^{+} CD8^{+} T cells secreting IFN-γ. *$P < 0.05$, **$P < 0.01$, ***$P < 0.001$, Mann-Whitney test.

in both nhTA^{+} and nhTA^{–} recipient chimeras with almost identical kinetics (Supplemental Figure 2). However, by day 60, significant differences in the functions of the remaining donor T cells had emerged. Thus, the level of in vivo cytotoxicity against antigen-expressing target cells was more than 3-fold lower in nhTA^{+} compared with nhTA^{–} chimeras (Figure 2B). Associated with these differences in CTL function, CD45.1^{+} CD8^{+} cells in nhTA^{–} recipients retained the ability to produce IFN-γ following ex vivo TCR stimulation, whereas this function was reduced in nhTA^{+} hosts (Figure 2C). These assays both detected rapid, recall immunity and were not initiated by either naive T cells or nontransferred cells (Supplemental Figure 3). Thus, loss of recall immunity only occurred in the presence of nonhematopoietic antigen.

In association with these functional differences, we also observed significantly lower absolute numbers of CD45.1^{+} CD8^{+} cells in both LNs and BM of nhTA^{+} versus nhTA^{–} recipients (Figure 2D). In the spleen, differences between the groups trended in the same direction, but did not reach statistical significance (Figure 2D). When we examined the phenotype of residual CD45.1^{+} CD8^{+} cells in each cohort, it became clear that the difference in numbers between the

groups could be explained primarily by differences in the absolute numbers of central memory cells (Tcm; CD44^{hi}CD62L^{hi}), which were 5- to 6-fold lower in nhTA^{+} than nhTA^{–} recipients in both spleen and LN (Figure 2E and data not shown). Compared with other subsets, Tcm populations are characterized not only by superior expansion potential upon reexposure to antigen, but also by higher baseline turnover in response to homeostatic cytokines in the absence of antigen (25, 35). To examine this latter property, we performed additional experiments in which we initially transferred Thy1.1^{+} SCs to nhTA^{–} hosts and CD45.1^{+} SCs to nhTA^{+} hosts. After 60 days, we sorted Thy1.1^{+} and CD45.1^{+} CD8^{+} cells from each group, mixed them at a 1:1 ratio, and cocultured them ex vivo with various cytokines. As shown in Figure 2F, there was a competitive disadvantage for the CD45.1[+] compared to the Thy1.1[+] population alone and in response to IL-15 and IL-7, consistent with defective memory homeostasis in nhTA^{+} recipients. Taken together, the data in Figures 1 and 2 indicate that persistent antigen expression within nonhematopoietic tissues impairs CD8^{+} memory function and homeostasis.

Loss of CTL function following DLI results from exhaustion. We reasoned that the failure to establish an effective memory pool in
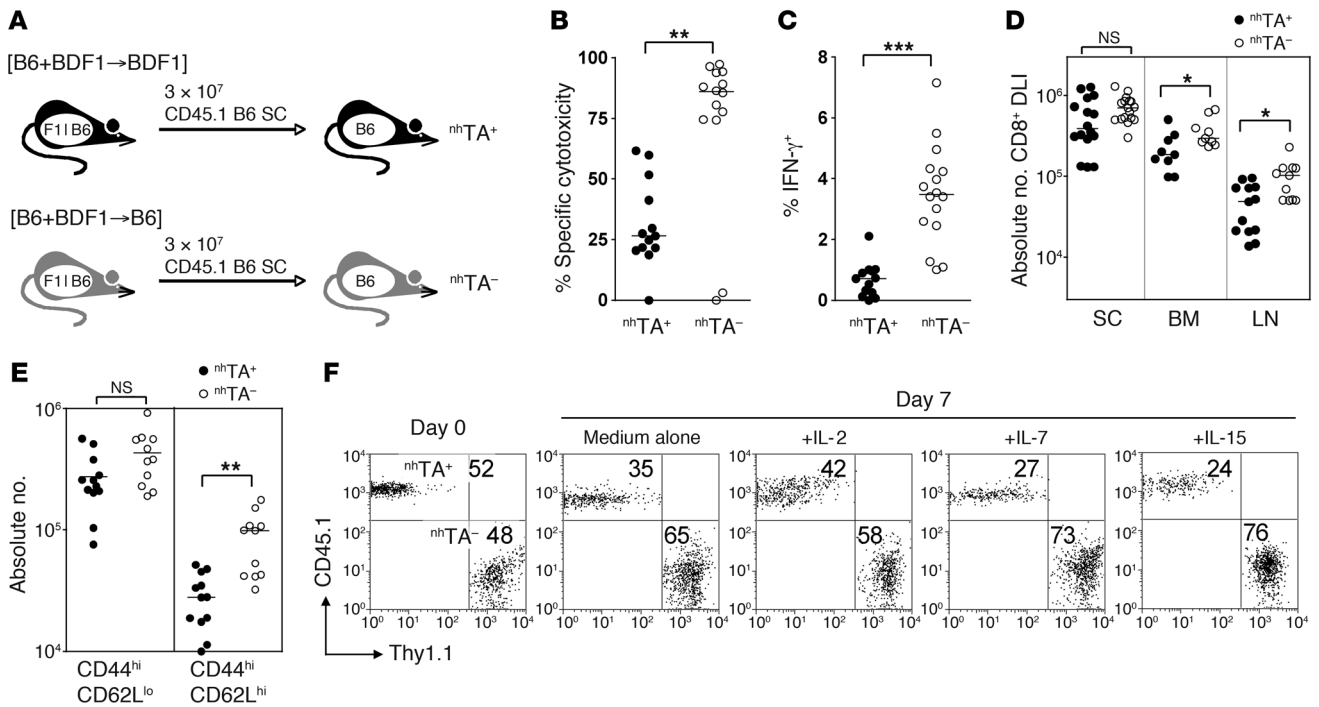
Figure 2
Nonhematopoietic antigen disrupts memory function and homeostasis. (**A**) nhTA+ [B6+BDF1→BDF1] and nhTA− [B6+BDF1→B6] allogeneic chimeras were established and 10 weeks later received 3 × 10⁷ CD45.1+ B6 SCs. (**B**) In vivo cytotoxicity of CFSE-labeled BDF1 target B cells 60 days after SC transfer. (**C**) IFN-γ production by CD45.1+ CD8+ T cells recovered from the spleens of recipients 60 days after SC transfer, following overnight stimulation with irradiated BDF1 SCs. (**D**) Absolute number of DLI-derived CD8+ T cells in the spleen, LN, and BM 60 days after SC transfer. (**E**) Scatter plots show the absolute number of CD44hiCD62Llo and CD44hiCD62Lhi DLI-derived CD8+ cells recovered from spleen. *P < 0.05, **P < 0.01, ***P < 0.001, Mann-Whitney test. (**F**) SCs (3 × 10⁷) were transferred from CD45.1+ and Thy1.1+ B6 mice to nhTA+ and nhTA− chimeras, respectively. At 60 days after transfer, CD8+ T cells were sorted by magnetic selection, mixed at a 1:1 ratio, and incubated in medium alone or with the indicated cytokines. Plots show starting mixture and the relative survival (as a percentage) of CD8+ T cells from nhTA+ or nhTA− hosts after 7 days culture.

nhTA+ hosts might derive from chronic TCR stimulation by non-hematopoietic cells bearing host MHC class I alloantigen, leading to their eventual exhaustion. To test this concept, we first examined the phenotype of residual CD45.1+ CD8+ cells at 60 days following transfer. Consistent with the concept of CTL dysfunction resulting from exhaustion in nhTA+ chimeras, the remaining donor CD8+ T cell population at day 60 expressed an IL-7 receptor α–low, programmed death-1–high (IL-7Rα^loPD-1^hi) phenotype (Figure 3A), typical of the signature observed in models of effector T cell dysfunction following chronic antigen exposure (22). In contrast, CD8+ cells recovered from nhTA− hosts were mostly IL-7Rα^hi and expressed markedly lower levels of PD-1 (Figure 3A). Furthermore, consistent with other models of CD8+ cell exhaustion (22), in vivo administration of anti–PD-L1 antibody partially restored the function of the donor CD8+ population. Thus, anti–PD-L1 treatment from day 48 to day 60 following donor T cell transfer significantly enhanced proliferation of CD45.1+ CD8+ cells in vivo, as determined by BrdU incorporation; increased the absolute numbers (but not frequency) of CD45.1+ CD8+ IFN-γ+ cells; and improved the levels of in vivo cytotoxicity against alloantigen-positive target cells (Figure 3, B–D). Importantly, although treatment with anti–PD-L1 antibody led to restoration of the antihost CD8+ response, recipient mice remained completely well, with no clinical or histological evidence of GVHD (Figure 3E).

Taken together, these data suggest that loss of CD8 function following transfer of donor T cells to allogeneic chimeras derives, at least in part, from exhaustion. Furthermore, anti–PD-L1 treatment at this stage led to significant reversal of CD8 dysfunction without leading to GVHD.

Direct antigen presentation is sufficient to induce CTL exhaustion. Because the initial alloresponse in this model required direct priming, we reasoned that exhaustion would be dependent upon stimulation of the CD8 TCR via direct recognition of allogenic MHC class I alloantigen upon nonhematopoietic cells. To test this, we performed similar transfer experiments in which we included 2C Tg CD8+ cells, which express TCR with high affinity for intact L^d class I alloantigen (36, 37) — thus, chronic stimulation could only be via direct presentation. Cells bearing the appropriate TCR could be tracked using a clonotypic marker. We therefore transferred 3 × 10⁷ CD45.1+ B6 SCs and 2 × 10⁶ purified 2C CD8+ cells to established nhTA+ [B6+BDF1→BDF1] chimeras. As before, host hematopoietic cells were eradicated by the initial GVH response (data not shown). 2C CD8+ cells were evident at both day 12 and day 60 (Figure 4A), confirming our previous findings that alloantigen-specific T cells are maintained within the repertoire at later time points (17). After 60 days, 2C CD8+ T cells expressed a similar CD44hiIL-7Rα^loPD-1^hi phenotype (Figure 4B), as observed previously in polyclonal donor CD8+ cells. Furthermore, ex vivo treatment with blocking antibodies
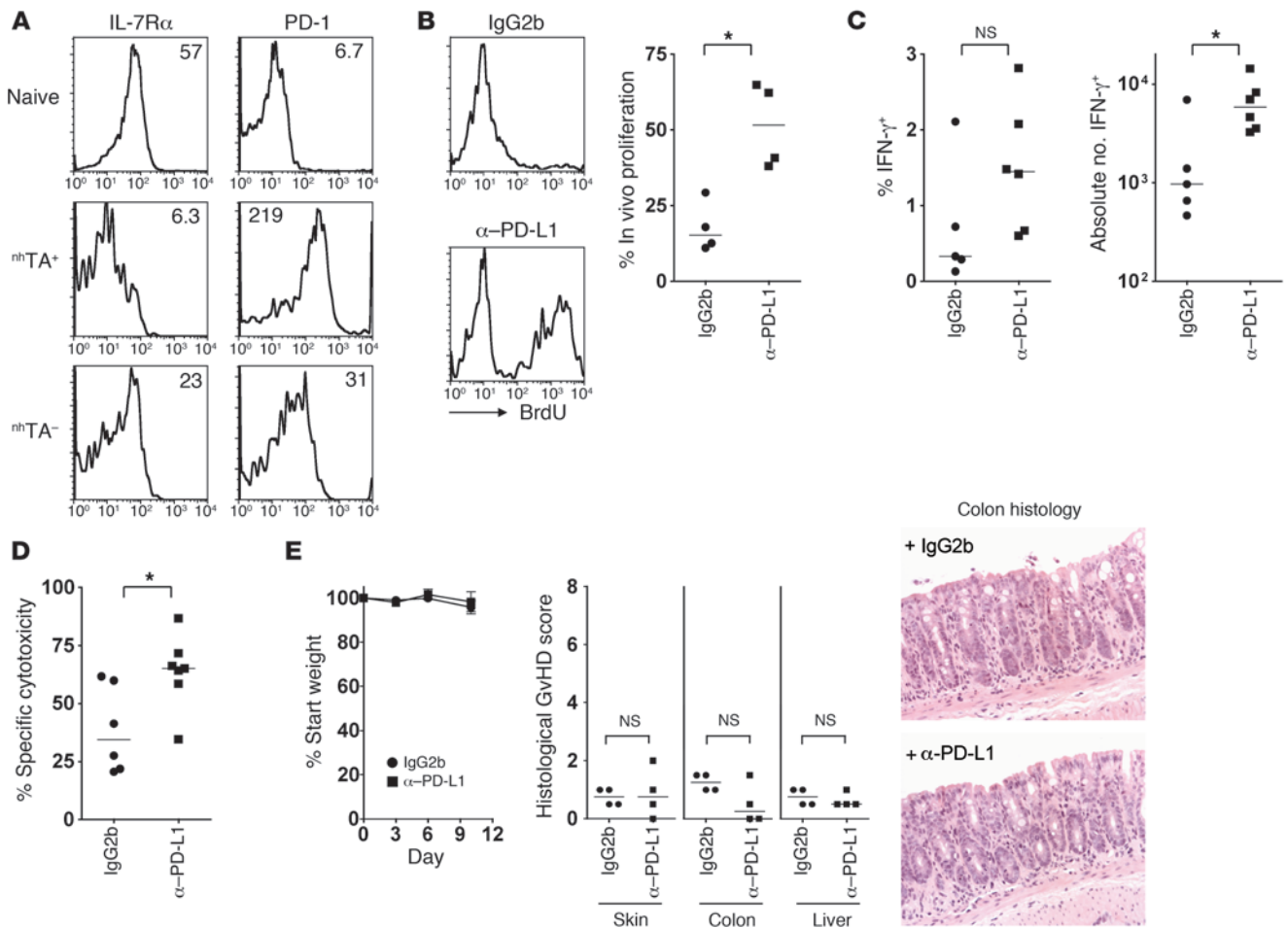
Figure 3
Function of exhausted CD8+ T cells can be partially restored by blockade of the PD-1/PD-L1 pathway. (**A**) Representative histograms show cell surface expression of IL-7Rα and PD-1 on spleen CD45.1+ CD8+ T cells of nhTA+ or nhTA− chimeras 60 days after SC transfer. Numbers indicate MFI: IL-7Rα, nhTA+ 20 ± 2 versus nhTA− 61 ± 4, $P < 0.001$, $n = 7$ per group; PD-1, nhTA+ 134 ± 16 versus nhTA− 29 ± 3, $P < 0.001$, $n = 13$–17 per group. (**B**–**E**) From 48 to 60 days after CD45.1+ B6 SC transfer, mice were administered 0.2 mg anti–PD-L1 or isotype control antibody by i.p. injection every 72 hours and received BrdU in the drinking water during the same period. (**B**) Representative histograms and summary data showing the percentage of CD45.1+ CD8+ T cells in the spleen that incorporated BrdU. (**C**) Summary data showing IFN-γ production at 60 days by CD45.1+ CD8+ splenic T cells after overnight stimulation with irradiated BDF1 SCs. (**D**) In vivo cytotoxicity of CFSE-labeled BDF1 target B cells. (**E**) Weight change; histological GVHD scores in skin, colon, and liver (scored single-blind); and representative colon histology (original magnification, ×200). Data are representative of 3 independent experiments. *$P < 0.05$, Mann-Whitney test.

to PD-L1 at day 60 improved the effector cytokine and proliferative functions of 2C CD8+ cells in nhTA+ recipients (Figure 4, C and D). Thus, direct presentation of antigen by nonhematopoietic cells is sufficient to induce exhaustion.

The effect of nonhematopoietic antigen upon CD8+ cell responses against a minor histocompatibility antigen. We next considered whether donor CD8 exhaustion also occurs in the context of responses following DLI in an MHC-matched, but minor histocompatibility (H) antigen–mismatched setting (similar to HLA-identical transplantations in humans). In mice, minor H antigen mismatches alone are insufficient to prime a quantifiable CD8 response under conditions in which DLI is given after 4 weeks (7, 16); thus, most protocols transfer cells at 1–3 weeks after BMT (7, 18, 38, 39). We first examined the fate of cells specific for a ubiquitous minor H antigen by transferring MataHari (Mh) Tg CD8+ cells bearing a TCR specific for a male antigen (UTY) presented in the context of

Db (HYDb-*Uty*; ref. 40). Although immediate transfer of Mh CD8+ cells to lethally irradiated B6 male mice induced severe GVHD (P. Reddy, unpublished observation), this did not occur when DLI was given 7 days following BMT, despite substantial expansion of the donor T cells. We therefore transferred $1 × 10^6$ Thy1.1 Mh CD8+ cells and $8 × 10^6$ polyclonal B6 female CD3 cells (to provide a helper response) 7 days following reconstitution of lethally irradiated B6 male mice with female B6 BM. Mh CD8+ cells (expressing the Thy1.1 marker and Vβ8.3; ref. 40) were readily identified in recipient secondary lymphoid organs at both day 7 and day 42 following transfer (Figure 5A). At day 7, a high frequency of Mh CD8+ cells produced IFN-γ upon brief ex vivo stimulation with UTY peptide (Figure 5B), 2- to 3-fold greater than Mh cells transferred to [B6 female→B6 female] syngeneic controls (data not shown). However, by day 42 following DLI, the frequencies of IFN-γ–producing cells were substantially diminished (Figure 5B). As in the case of partially MHC-
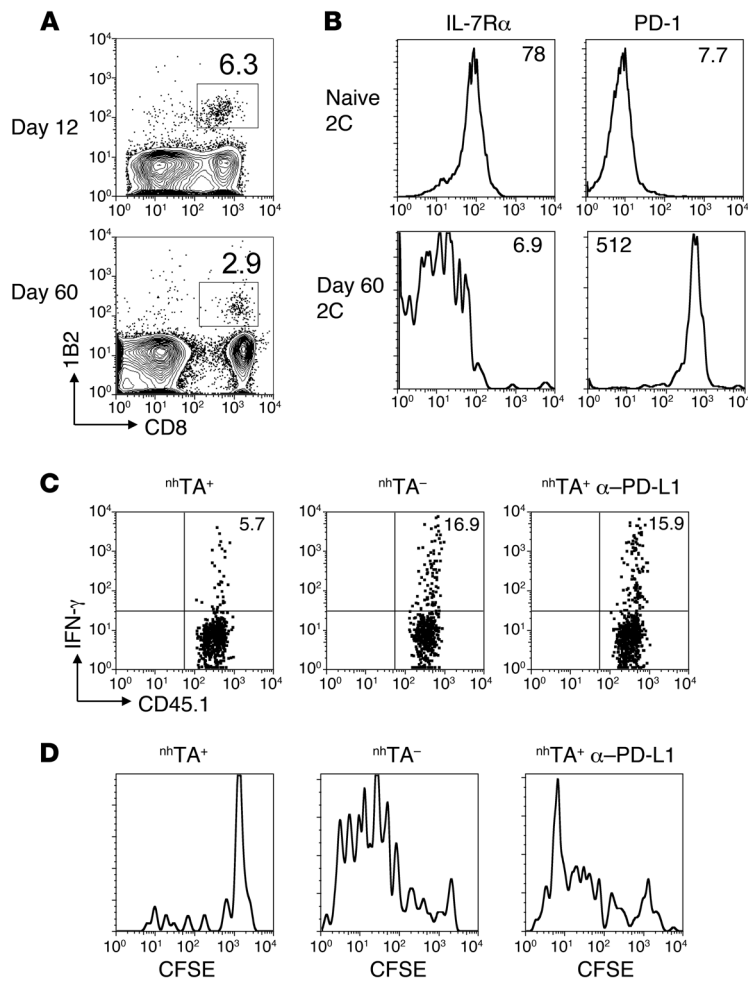
Figure 4
Direct recognition of antigen upon nonhematopoietic antigen is sufficient to drive exhaustion of transferred CD8+ T cells. B6 SCs (3×10^7) in combination with 2C Tg CD45.1+ CD8+ T cells (2×10^6) were transferred to established nhTA+ chimeras. (**A**) Contour plots showing frequency of 1B2+ cells as a percentage of CD8+ cells in spleen at 12 and 60 days after transfer to nhTA+ recipients. (**B**) Histograms show cell surface phenotype of 2C Tg CD8+ T cells (gated using 1B2 clonotypic antibody) from nhTA+ mice at 60 days following transfer. (**C**) SCs recovered from nhTA+ or nhTA− chimeras 60 days after transfer were stimulated overnight with irradiated BDF1 SCs in the presence of isotype control or anti–PD-L1 blocking antibody. Representative dot plots show IFN-γ production by 2C Tg CD8+ T cells (Tg cells were on a CD45.1 background in this experiment). (**D**) Representative histograms show ex vivo proliferation (in the presence of control or anti–PD-L1 blocking antibody) of 2C CD8+ T cells recovered from the spleen 60 days following transfer to nhTA+ or nhTA− chimeras. Data derived from 2 independent experiments with similar results ($n = 2–3$ mice per group).

mismatched chimeras, late in vivo anti–PD-L1 treatment increased in vivo proliferation of Mh CD8+ cells and substantially enhanced the number of IFN-γ–producing cells (Figure 5, B and C). Furthermore, despite the dramatic improvements in the functionality of Mh cells, anti–PD-L1 treatment did not induce either clinical or histological GVHD (Figure 5D and data not shown).

Following the initial phase of the response, Mh effector cells could theoretically encounter HYD[b]-*Uty* complexes presented either directly by nonhematopoietic cells or cross-presented by female donor BM-derived APCs. To determine the involvement of direct presentation by nonhematopoietic cells upon the development of the exhausted Mh phenotype, we explored the fate of primed cell populations upon transfer to hosts where nonhematopoietic cells either could or could not present antigen directly. Thus, 7 days following DLI (as in Figure 5), activated T cells from recipient spleens were transferred to either [B6 female→B6 male] or [B6 female→β_2m$^{-/-}$ male] chimeras (referred to herein as [F→M] and [F→β_2m$^{-/-}$M], respectively), and the functions of the transferred cells were examined 21 days later (Figure 6A). In [F→M] chimeras, UTY antigen could be presented directly by nonhematopoietic cells or cross-presented by female BM-derived cells, whereas in [F→β_2m$^{-/-}$M] chimeras, which lack surface MHC class I expression on nonhematopoietic tissues, UTY antigen could only be cross-presented. At both day 8 and day 20 following secondary transfer, we observed significant decreases in PD-1 expression by

Mh cells in the peripheral blood of [F→β_2m$^{-/-}$M] compared with [F→M] chimeras, although the differences were not large (Figure 6B). To detect PD-1 expression in these experiments, we used the J43 anti–PD-1 antibody, which has a fairly narrow range of expression in exhausted CD8+ cells (41). Thus, to further discriminate cell populations with potentially differing levels of exhaustion, we examined coexpression of PD-1 with CD44, since it has previously been demonstrated following chronic viral infection that cells with greater levels of dysfunction lose expression of CD44, especially within the BM compartment (41). Indeed, in the BM of [F→M] chimeras at day 21, the major Mh population was PD-1hiCD44int/lo, consistent with a terminally exhausted phenotype (41). In contrast, in the BM of [F→β_2m$^{-/-}$M] chimeras, the PD-1hiCD44int/lo population was significantly smaller, and the frequency of cells expressing PD-1 was lower (Figure 6C). In the spleen, the predominant Mh population was PD-1intCD44hi in both sets of chimeras, although the frequency of cells expressing PD-1 was again lower in [F→β_2m$^{-/-}$M] chimeras. Consistent with reduced exhaustive stimuli under conditions in which nonhematopoietic cells cannot present antigen directly, the frequency of IFN-γ–producing Mh cells was also significantly higher in [F→β_2m$^{-/-}$M] versus [F→M] chimeras (Figure 6D). Taken together, these data suggest that direct presentation of a minor H antigen by nonhematopoietic cells contributes to the development of CD8 exhaustion following DLI. Furthermore, they reaffirmed that the functions of
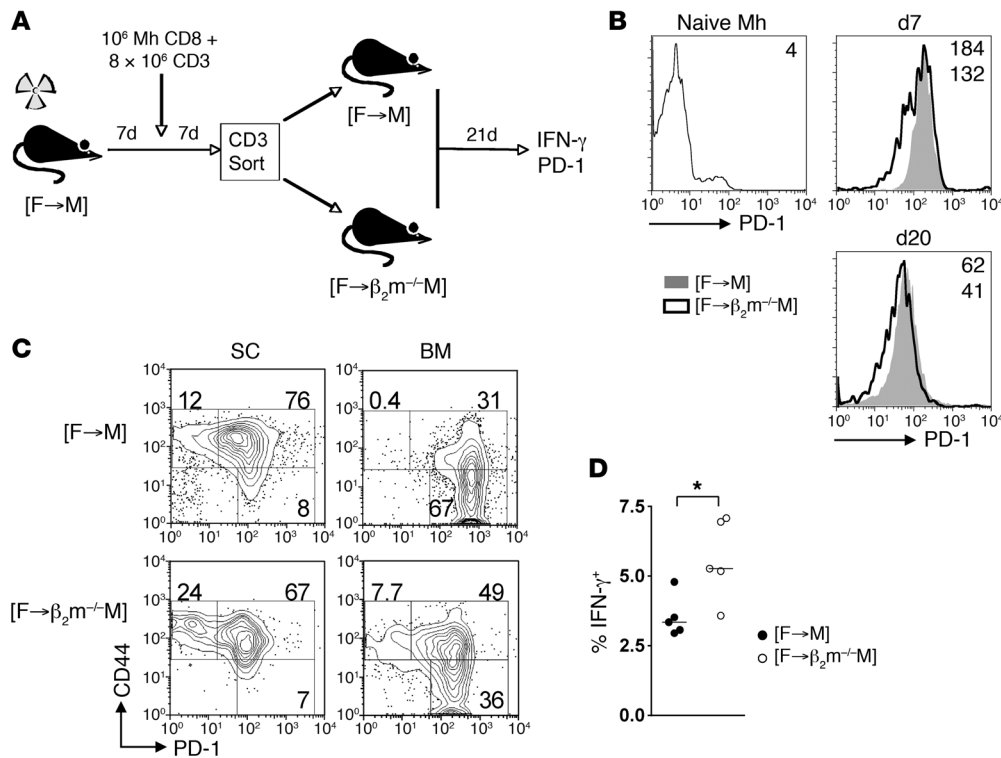
Figure 5
Minor H antigen–specific CD8+ T cells recognizing ubiquitously expressed host antigens are susceptible to exhaustion. B6 female CD3 cells (8×10^6) and Mh Tg Thy1.1+ CD8+ cells (10^6) were transferred 1 week after lethal irradiation of B6 male mice and reconstitution with female B6 BM. At 36 and 39 days following T cell transfer, mice were administered 0.2 mg anti–PD-L1 blocking antibody or isotype control by i.p. injection and received BrdU in the drinking water during the same period. (**A**) Representative contour plots showing frequency of Thy1.1+ CD8+ cells as a percentage of SCs. (**B**) SCs recovered from chimeras at 7 or 42 days after T cell transfer were stimulated overnight with UTY or irrelevant peptide. Representative dot plots and summary data show IFN-γ production by CD8+ Thy1.1+ Mh T cells. Gates set according to irrelevant peptide. (**C**) Representative histograms and summary data showing the percentage of Thy1.1+ CD8+ T cells incorporating BrdU. (**D**) Single-blind scoring of histological GVHD in sections taken from skin, colon, and liver of recipient mice. Data derived from 4 independent experiments. **$P < 0.01$, Mann-Whitney test.

exhausted cells can be partially restored by late anti–PD-L1 treatment without the induction of GVHD.

Nonhematopoietic antigen blocks early generation of postmitotic, CD62L+ CD8+ cells. Although our findings demonstrated that exhaustion of chronically stimulated donor CD8+ cells contributes to failure to establish competent recall immunity following DLI, we also considered how antigen expression by nonhematopoietic tissues influences the primary CD8 response. Using the same partially MHC-mismatched experimental system as in Figure 2, we observed distinct patterns of donor cell accumulation by day 12–14 of the DLI response, with greater CD8+ cell numbers in the spleens of nhTA+ chimeras but a reciprocal pattern in the LNs, where numbers were 3-fold higher in nhTA– chimeras (Figure 7A). At this early time point, there was also a significant divergence in the effector competence of the transferred CD8+ cells. Although there were minor differences in cytotoxicity against allogenic target cells (with a minor reduction in nhTA+ hosts), the capacity of nhTA+ CD8+ cells to produce IFN-γ at the peak of the response was 3-fold lower (Supplemental Figure 4). This limitation of effector cytokine generation in nhTA+ hosts was

independent of extrinsic control by regulatory T cell populations (14, 42), as neither depletion of CD25+ cells nor selective in vivo depletion of the endogenous T cell compartment enhanced IFN-γ synthesis in nhTA+ chimeras (Supplemental Figure 4).

These early differences in intrinsic effector function were associated with distinct phenotypic profiles of proliferating cells. Thus, although the rates of proliferation (as detected by CFSE dilution) were very similar in both sets of chimeras, with the vast majority of donor CD8+ cells undergoing extensive division by day 8, the proportion of postmitotic, CFSElo donor CD8+ cells that retained CD62L expression was more than 3-fold greater in the nhTA– cohort (Figure 7B). Furthermore, on dual staining, the proportion of postmitotic, CD8+ cells that had a Tcm-like CD44hiCD62Lhi phenotype was also greater in nhTA– chimeras, whereas cells with a CD44hiCD62Llo effector phenotype predominated in the nhTA+ group (Figure 7, C and D). This excess of postmitotic, Tcm-like cells in nhTA– chimeras was even more pronounced in the LNs and was also evident in the BM (Figure 7C). These differences in the frequencies of postmitotic CD44hiCD62Lhi cells between

Figure 6
Direct presentation of a minor H antigen by nonhematopoietic cells contributes to exhausted phenotype. (**A**) B6 female CD3+ (8 × 10^6) and Mh Tg female CD8+ (10^6) cells were transferred 1 week after lethal irradiation of B6 male mice and reconstitution with female B6 BM. 7 days following DLI, T cells were isolated from spleen of primary recipients, and 13 × 10^6 CD3+ cells (containing 5 × 10^6 Mh cells) were transferred to [F→M] or [F→β2m−/−M] chimeras on the basis of 1 donor spleen equivalent to 1 secondary recipient (*n* = 5 per group). Secondary chimeras were set up at the same time as the primary recipients. (**B**) Representative overlay histograms of surface PD-1 expression upon naive Mh cells and in peripheral blood at 8 and 20 days following secondary transfer. Numbers indicate MFI (top, [F→M] or naive; bottom, [F→β2m−/−M]); day 8, [F→M] 180 ± 7 versus [F→β2m−/−M] 130 ± 7 (*P* < 0.01); day 20, 58 ± 3 versus 40 ± 1 (*P* < 0.01). (**C**) Representative contour plots showing PD-1 and CD44 expression in gated Mh cells within spleen and BM at day 21 following secondary transfer. Figures denote proportion of Mh cells within each gate: spleen, PD-1^lo cell frequency [F→M] 14% ± 2% versus [F→ β2m−/−M] 22% ± 1% (*P* < 0.01); BM, PD-1^hiCD44^int/lo cell frequency 61% ± 2% versus 43% ± 1% (*P* < 0.01); BM, PD-1^lo cell frequency 1% ± 0.3% versus 7% ± 0.8% (*P* < 0.01). (**D**) Summary data of frequency of IFN-γ generation by Mh CD8+ cells following stimulation with UTY peptide. (**B–D**) 1 of 2 independent experiments with similar results. *P* < 0.05, Mann-Whitney test.

with enhanced recruitment of functional CD8+ effectors to peripheral tissues (Supplemental Figure 6). Taken together, these data indicate that initial, direct recognition of alloantigen upon nonhematopoietic cells blocks the generation of postmitotic, CD62L^hi CD8+ cells.

Nonhematopoietic antigen blocks early memory imprinting. Recent studies in mice have revealed that postmitotic, CD62L+ cells with effector functions can arise early during the primary response (6, 26, 43), and, in some cases, may have the potential for self renewal (6, 43). One possible interpretation of the above data was that nonhematopoietic antigen blocks memory imprinting during priming and thus further contributes to the failure of recall immunity in the long term. To test this concept, we performed adoptive transfers to ^nhTA+ or ^nhTA− chimeras, similar to the experiments described in Figure 2, and then examined the fate of purified CD8+ cells upon secondary transfer to an antigen-free host. This approach enabled us to test the ability of transferred cells to be maintained in the absence of antigen and to mount a recall response, hallmark properties associated with memory establishment. In these experiments, we used CD45.1+ and CD45.1+CD45.2+ B6 donors in ^nhTA+ and ^nhTA−

the groups were also observed following transfer of flow-sorted, CD44^loCD62L^hi naive polyclonal T cells (data not shown), excluding the preferential accumulation of preexisting memory phenotype cells as an explanation for the difference. Furthermore, naive 2C CD8+ cells transferred to ^nhTA+ also showed a relative failure to differentiate into a Tcm-like population following initial priming (Supplemental Figure 5), which demonstrated that these differences occurred as a result of early, direct recognition of alloantigen upon nonhematopoietic cells. Although expansion of this Tcm-like population was blocked by nonhematopoietic antigen, this effect appeared to be independent of coinhibition via the PD-1/PD-L1 pathway. Thus, early in vivo anti–PD-L1 antibody blockade instead drove terminal differentiation of donor CD8+ cells and further loss of the CD44^hiCD62L^hi population (Figure 7F). Furthermore, and in sharp contrast to late treatment, early in vivo anti–PD-L1 treatment induced clinical and histological GVHD, consistent

recipients, respectively. At the peak of the response, we sorted CD45.1+ CD8+ cells from the spleen of each cohort, mixed them at a 1:1 ratio, and transferred a total of 6 × 10^6 purified cells to secondary hosts that lacked alloantigen in both BM-derived and peripheral tissues (established CD45.2+ B6→B6 chimeras), as outlined in Figure 8A. At this time point, no differences were observed in the proportion of cells that were annexin V+ (^nhTA+, 60.1% ± 3.4%; ^nhTA−, 54.2% ± 1.2%; *P* = NS). At 7 days following secondary transfer, the frequency of CD8+ cells derived from primary ^nhTA− and ^nhTA+ hosts was equivalent in peripheral blood (Figure 8B), thus demonstrating similar levels of initial engraftment. However, thereafter, the relative frequency of cells derived from ^nhTA+ primary hosts declined compared with those from ^nhTA− primary hosts. At day 14, secondary recipients were immunized with LPS-activated BDF1 DCs, and the recall response was determined 7 days later (Figure 8A). By day 21, 2- to 3-fold fewer ^nhTA+ primary
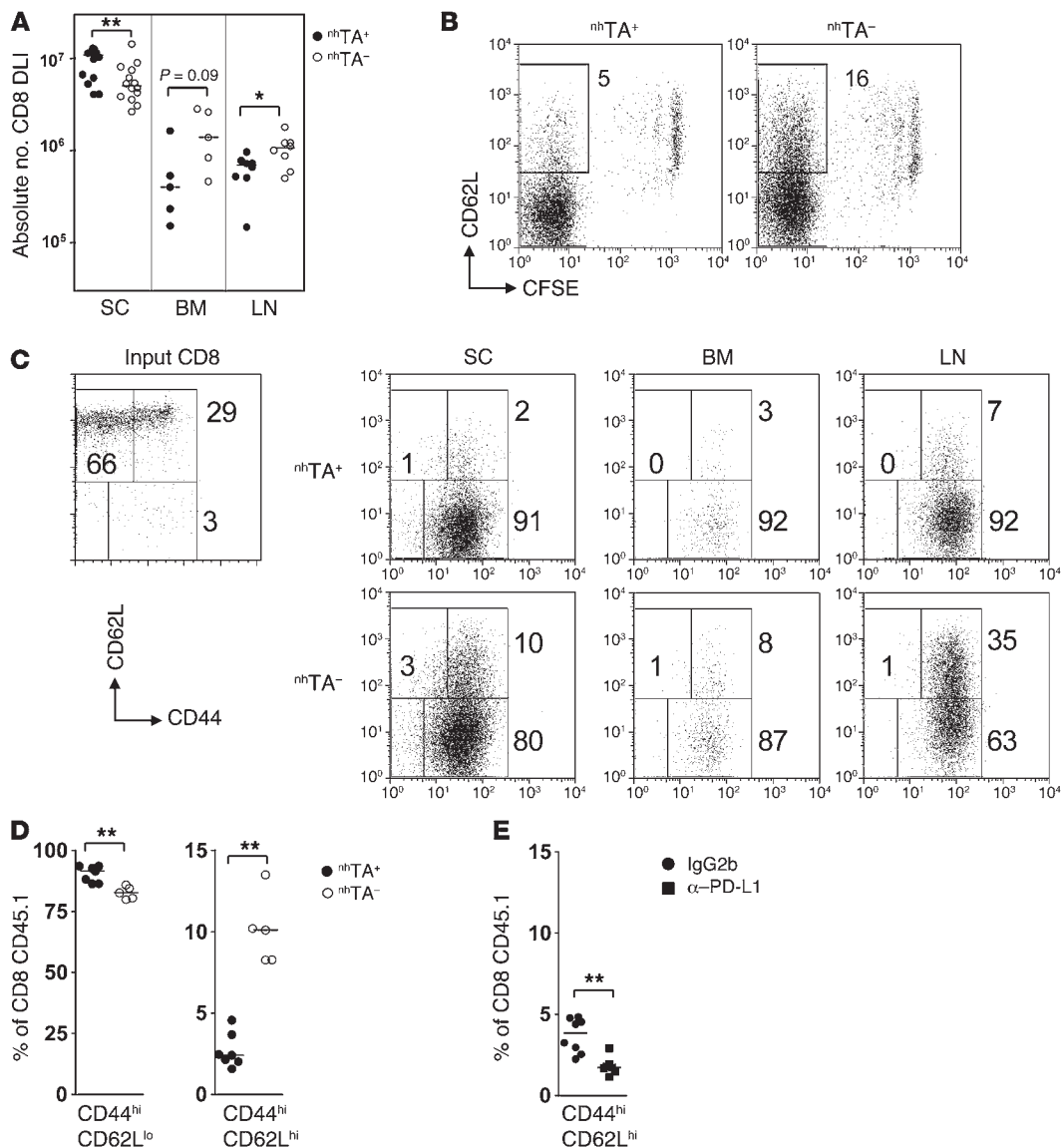
Figure 7
Nonhematopoietic antigen blocks early generation of postmitotic, CD62L$^+$ CD8$^+$ cells. (**A**) CD45.1$^+$ B6 SCs (3 × 10^7) were transferred to established allogeneic chimeras as in Figure 2. Accumulation of DLI-derived CD8$^+$ T cells in the spleen, LN, and BM in ^{nh}TA$^+$ and ^{nh}TA$^-$ recipients 14 days after transfer is shown. (**B**) Representative dot plots showing CFSE versus CD62L staining in the CD45.1$^+$ CD8$^+$ gated population at day 8. Numbers denote percent CD8$^+$ CFSE^{lo} cells that were CD62L$^+$. (**C**) Representative dot plots showing CD44 and CD62L staining in input CD8$^+$ cells and in CFSE^{lo} CD45.1$^+$ CD8$^+$ gated population. (**D**) Summary data for the same gated population in spleen. Significant differences were also evident in the LN and BM (not shown). (**E**) ^{nh}TA$^+$ chimeras received a transfer of 3 × 10^7 B6 CD45.1$^+$ SCs followed by i.p. injection of 0.2 mg anti–PD-L1 antibody on days 0, 3, 6, and 9. At 12 days, the proportion of CD45.1$^+$ CD8$^+$ gated cells with a CD44^{hi}CD62L^{hi} phenotype was determined. Data derived from 3 independent experiments. *P < 0.05, **P < 0.01, Mann-Whitney test.

CD8$^+$ cells compared with ^{nh}TA$^-$ primary CD8$^+$ cells were recovered from the blood and spleen of the secondary hosts (Figure 8, B and C). Although a substantial proportion of the CD8$^+$ cells derived from ^{nh}TA$^+$ hosts were able to generate IFN-γ, there was a trend for a lower capacity to do so on a per-cell basis compared with cells derived from ^{nh}TA$^-$ hosts (Figure 8, D and E); this was nearly 4-fold lower when compared in terms of absolute CD8$^+$ IFN-γ$^+$ numbers (Figure 8E). This failure of cells from ^{nh}TA$^+$ chimeras to fully establish recall immunity in antigen-free hosts was associated with reduced frequencies of both CD62L^{hi} and IL-7Rα^{hi} CD8$^+$

memory populations (Figure 8F), equating to an approximately 6- to 7-fold reduction in their respective absolute numbers. Taken together, these data indicate that priming in the presence of nonhematopoietic antigen blocks memory imprinting during the initial stages of the response, severely impairing the establishment of memory populations in the absence of antigen.

Discussion

In this study, we have shown that antigen within nonhematopoietic tissues is not ignored, but rather actively shapes the long-term
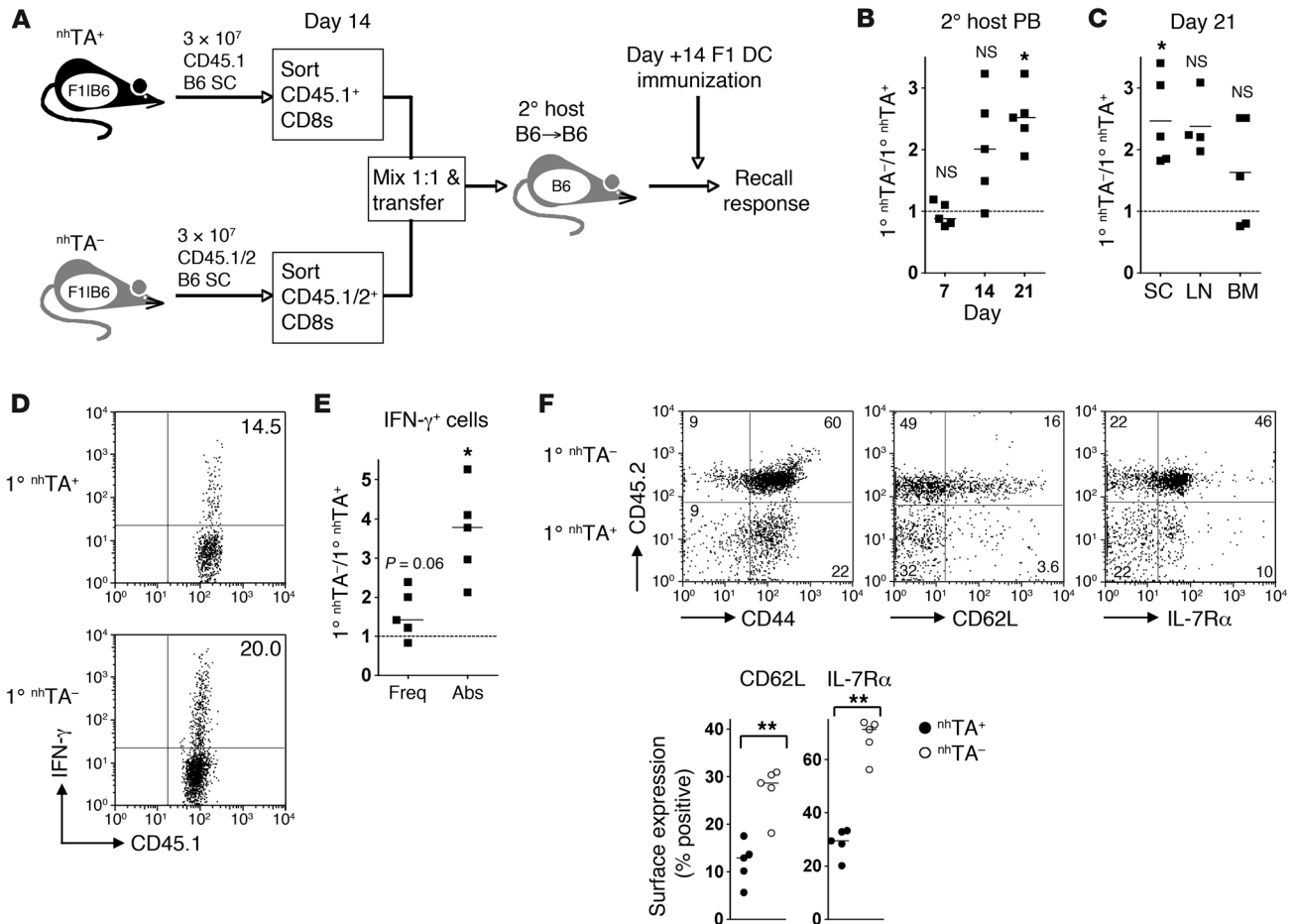
Figure 8
Nonhematopoietic antigen regulates early memory fate determination. (**A**) CD45.1+ or CD45.1/2+ B6 SCs (3 × 10^7) were transferred to nhTA+ and nhTA− chimeras, respectively. 14 days later, CD45.1+ CD8+ T cells from nhTA+ and nhTA− chimeras were sorted, mixed at a 1:1 ratio, and transferred to established secondary B6→B6 hosts. After 14 days, secondary hosts were immunized i.p. with 1 × 10^6 BDF1 LPS-matured DCs, and recall immunity was measured 7 days later. (**B**) Relative frequency of the 2 transferred CD8+ T cell populations in the blood of secondary hosts at timed intervals following secondary transfer (ratio of CD45.1+CD45.2+ to CD45.1+CD45.2− CD8+ cells). (**C**) Relative frequency of above populations in the spleen, LN, and BM of secondary hosts at 21 days. (**D**) Representative plots show IFN-γ production by CD45.1+ CD8+ T cells that were CD45.2− (nhTA+) or CD45.2+ (nhTA−). (**E**) Summary data showing the relative function in terms of the frequency (freq) and absolute number (abs) of CD8+ T cells producing IFN-γ. (**B**, **C**, and **E**) *P < 0.05, Wilcoxon signed rank test relative to expected ratio of 1 (dotted line). (**F**) Representative dot plots show the cell surface expression of CD44, CD62L, and IL-7Rα on CD8+ CD45.1+ cells 21 days following secondary transfer. Numbers indicate the percentage of gated cells in each quadrant. Scatter plots show the percentage of each transferred cell population expressing cell surface markers. **P < 0.01, Mann-Whitney test.

integrity of CD8+ T cell immunity. In a model of delayed DLI following allogeneic BMT, we found antigen expression within the nonhematopoietic compartment to impair long-lasting immunity at 2 distinct levels: first, it critically impaired the early imprinting of CD8+ memory differentiation; second, it drove exhaustion of surviving CD8+ cells via direct recognition. These 2 factors, in concert, contribute to an even more profound failure to provide effective immunosurveillance. Importantly, the functions of exhausted CD8+ cells were reversed by late PD-1/PD-L1 blockade without induction of GVHD, suggestive of a potential clinical strategy to prevent or treat tumor relapse following allogeneic BMT.

The negative regulatory effect of nonhematopoietic tissues upon memory precursor programming was associated with a distinct block in the generation of postmitotic, CD62L^hi CD8+ cells in the primary response. Within other experimental systems, Tcm-like

populations have also been reported to arise early in the response, which suggests that memory differentiation can occur in a non-linear fashion, without passing through a full effector stage (6, 26, 43, 44). The factors influencing early fate determination of CD8+ cells are complex and likely to be multifactorial. Existing concepts have highlighted the role of inflammation (27), the initial antigen load (45, 46), the quality (47) and duration (28) of stimulation, and the extent of clonal competition (48) in dictating the long-term memory potential of antigen-reactive CD8+ T cells. Each of these factors might also be relevant in the case of nonhematopoietic antigen, although in the present study we invoked direct presentation, rather than cross-presentation, of antigen as being the relevant factor. For example, ubiquitous antigen expression may prolong stimulation during the initial stage of the response (28) or effectively reduce clonal competition (48), skewing activated CD8+

T cell differentiation away from memory precursor formation. Alternatively, the quality of antigen presentation by nonhematopoietic cells may be important, since weak or transient immune synapse formation is linked to impaired memory establishment (47, 49). Although synapse formation between nonhematopoietic cells and donor T cells might potentially involve greater interaction between coinhibitory ligands and their receptors, our finding that PD-L1 blockade drove terminal rather than Tcm differentiation suggests that coinhibition via this pathway is not a crucial determinant of memory precursor differentiation. At the molecular level, the mechanisms that regulate early fate decisions in CD8+ cells are less well understood, although recent studies have suggested the involvement of the Blimp1/Bcl6 axis (50), the Wnt/β-catenin pathway (51), or the mammalian target of rapamycin pathway (52). In this regard, our initial evaluations of gene expression profiles of Tg antihost CD8+ cells activated in $^{nh}TA^+$ or $^{nh}TA^-$ chimeras have not demonstrated differences in the expression of target genes regulated by each of these pathways (B. Flutter and S. Henderson, unpublished observations), which suggests that nonhematopoietic antigen influences memory precursor generation by distinct mechanisms. Delineation of such mechanisms may be important in devising strategies to overcome the block in early memory precursor generation that contributes to loss of effective recall immunity.

In the longer term, peripheral antigen progressively impairs the performance of surviving CTL, and cells with this impairment eventually become exhausted. Although models of exhaustion — as in the present study — require the persistence of antigen (53), additional factors during the very early stages of CD8+ cell differentiation may also influence the extent of this outcome. One critical factor is the extent of CD4 help provided during the priming response (54). The CD8 response in the MHC-mismatched model is helper dependent (11), and it is noteworthy that although the CD4 proliferative responses were robust, CD4 cells failed to produce copious amounts of Th1/2/17 cytokines via TCR stimulation at any stage (data not shown). This raises the question as to whether helper responses initiated in this model are relatively weak, rendering CD8+ cells effectively helpless and reducing the threshold for exhaustion (22). Against this concept, we have found that enhancement of CD4 responses at the time of priming using anti-OX40 agonistic costimulation does not prevent the long-term dysfunction of the CD8 response in the face of persistent nonhematopoietic antigen expression (B. Flutter et al., unpublished observations). Of note, in our partially MHC-mismatched experimental system, exhaustive differentiation of donor CD4 cells was not observed (Supplemental Figure 7). This protection from exhaustive differentiation can be explained by restriction of MHC class II alloantigen to hematopoietic cells that are cleared following the initial conversion to full donor chimerism. One intriguing, potentially related, clinical observation is that GVT responses are enhanced in the setting of isolated donor-recipient HLA-DPB1 mismatches (55). Since such mismatches are anticipated to involve an element of direct priming (55, 56), it is conceivable that responding donor CD4+ cells can escape exhaustion upon initial clearance of host hematopoietic elements or leukemia cells, and thus provide long-term immunosurveillance. This may also be of relevance to the strategy of CD8-depleted DLI in patients who have undergone haploidentical transplantation (57), as we infer from our present data that infused donor CD4+ cells would maintain their functions.

In contrast to antigen recognized by CD4+ cells, the ubiquitous and lasting expression of MHC class I alloantigen or class I–restricted minor H antigens in nonhematopoietic tissues drives the eventual exhaustion of CD8+ cells. Our data help to explain the mechanisms underlying the nondeletional, peripheral tolerance of CD8+ cells described in other experimental systems involving restriction of alloantigen expression to parenchymal cells (58). Our findings also explain the failure of GVT responses to be sustained in the long term following delayed transfer of donor T cells to allogeneic chimeras, despite the persistence of host-reactive T cells (17). In humans, GVT responses following DLI may include those specific for host class I–restricted minor H antigens whose expression is restricted to the hematopoietic system (e.g., HA-1 and HA-2; ref. 59). We reason that exhaustion will not occur under these circumstances, since host BM-derived cells — and hence the priming antigens — are eradicated. Indeed, when we tracked a DLI-derived CD8 response to H60, a minor H antigen whose expression is restricted to the hematopoietic system (60), IFN-γ responses were maintained in the long term, and late anti–PD-L1 antibody treatment had no effect upon the response (Supplemental Figure 8), which indicates that exhaustion of CD8+ cells with specificity for this host, hematopoietic-restricted minor H antigen, did not occur. These findings support the clinical approach of transfer of CD8+ cells selected for specificity to hematopoietic antigens such as HA-1. In contrast, our data suggest that antitumor responses directed at antigens with broader expression are more likely to fail. Indeed, persistent CD8 stimulation in this context may ultimately lead to replicative senescence, a profound and irreversible exhausted end state observed in both experimental and clinical studies (41, 61). However, exhaustion may not be the dominant process in the context of GVHD, where memory cells may continue to drive tissue injury (6, 62). In this situation, injury to peripheral tissues might enhance cross-presentation of host antigens and thus deliver more effective priming by donor BM-derived APCs (33). The capacity of donor BM-derived APCs to provide costimulation (25) or trans-present IL-15 (63) might be important additional factors in permitting ongoing generation of antihost memory cells to replenish exhausted effectors.

Importantly, donor CD8+ cell exhaustion can occur in the absence of GVHD, since exhausted CD8+ cells do not accumulate in extralymphoid tissues following delayed DLI (3). Although we cannot exclude the importance of low-level recirculation to these sites, we believe it is possible that the development of CD8 dysfunction occurs primarily within the lymphohematopoietic system, rather than within peripheral tissues. Candidate nonhematopoietic cells that might participate in disrupting the differentiation of effector CD8+ cells include stromal, epithelial, or vascular endothelial cells. For example, stromal cells within the lymphohematopoietic system may present antigen directly to T cells, as was originally proposed by Sprent and colleagues (64) and confirmed recently by others (65). The intimate association between T cells and the fibroblastic reticular network within LN and spleen (66) might therefore be of importance, particularly if such interactions involve cognate recognition. In this regard, chronic LCMV infection involves heavy infection of fibroblastic reticular cells in secondary lymphoid organs and their close approximation to antigen-specific T cells (67, 68). It will therefore be of interest to determine how this cell population influences initial programming and durable functions of CD8+ cells.

Although PD-1/PD-L1 blockade has been demonstrated recently to improve GVT responses limited by nonhematopoietic antigen

early after BMT (69), this occurs at the expense of severe GVHD, thus limiting its potential clinical application. Indeed, blocking the pathway during the very early phase of the DLI response not only led to GVHD, but also reduced the number of Tcm-like cells still further, suggestive of a very limited role for this strategy at the initiation of the response. In contrast, we found that PD-L1 blockade at late stages following DLI significantly restored antihost CTL function without induction of GVHD both in MHC-mismatched and in MHC-matched, minor H antigen–mismatched models. Our findings therefore suggest a clinical context in which blockade of the PD-1/PD-L1 pathway could potentially be performed safely in order to prevent or treat relapse following BMT. The finding that GVHD was induced when anti–PD-L1 was applied early could reflect the distinct roles of the PD-L1 upon hematopoietic and nonhematopoietic tissues (70). Thus, in the early phase of the response following DLI, PD-1/PD-L1 blockade would be anticipated to interrupt coinhibitory signaling to CD8+ cells from both nonhematopoietic cells and host BM-derived APCs, acting in concert to drive host injury. In contrast, when host hematopoietic elements have been eradicated, CD8+ cells would be less likely to receive costimulatory signals from host APCs that are important in the development of GVHD (71, 72).

In summary, our data demonstrated how nonhematopoietic alloantigen expression impedes both imprinting and maintenance of antihost CD8 memory following delayed DLI. While these effects might act together to limit the development of GVHD, they also have the potential to eventually impair durable GVT activity. From a therapeutic perspective, the development of strategies that target the interaction between CTL and nonhematopoietic cells may be of value in boosting weakened, long-term immunosurveillance against tumor. Our finding that late PD-1/PD-L1 blockade following delayed DLI restored the functions of exhausted CD8+ cells without inducing GVHD has important clinical implications.

Methods

Animals. Female B6, B6×DBA/2 (BDF1), and 129S2/SvPasCrlf mice were purchased from Charles River Laboratories. B6.SJL (CD45.1+) mice were purchased from the Frederick Cancer Research facility. B6.PL-Thya/Cy mice (Thy1.1+) and B6.129P2-β2mtm1Unc were purchased from The Jackson Laboratory and were then bred in house by UCL Biological Services. 2C TCR Tg mice (B6 background) were provided by D. Loh (Washington University, St. Louis, Missouri, USA; ref. 36) and bred onto B6.SJL background in house. Mh TCR Tg mice (40) on a B6.PL-Thya/Cy background were obtained from J. Dyson (Imperial College London, London, United Kingdom). All procedures were conducted in accordance with the United Kingdom Home Office Animals (Scientific Procedures) Act of 1986. The present experiments were reviewed and approved by the Ethics and Welfare Committee of the Comparative Biology Unit, Royal Free and University College London Medical School (London, United Kingdom).

PD-L1, Thy1.2, and CD25 antibodies. Anti-mouse PD-L1 (10F.9G2), anti-Thy1.2 (30H12), anti-CD25 (PC-61.5.3), and their respective isotype controls have been described previously (14, 73, 74).

BMT and DLI. BMT and subsequent DLI were performed as described previously (15). Recipient mice were lethally irradiated (B6 and BDF1, 11 Gy; 129, 9 Gy X-ray irradiation, 0.55 Gy/min split in to 2 fractions, separated by 48 hours) and T cell–depleted BM cells were injected intravenously 4 hours later. In MHC-matched, minor H antigen–mismatched BMT, no T cell depletion was used. In experiments to examine early in vivo proliferation of donor T cells, SCs were labeled with 2–5 μM CFSE (Sigma-Aldrich) prior to infusion. Uptake of BrdU was used to examine

the turnover of cells in vivo at later time points by administration of 0.8 mg/ml BrdU (Sigma-Aldrich) in the water of recipient mice over time periods specified in the text.

Secondary transfer and cytokine response experiments. T cells were isolated from individual or pooled SC suspensions of DLI recipients by negative selection to remove non-CD3+ or non-CD8+ cells (Pan T cell isolation or CD8+ T cell isolation kits; Miltenyi Biotec) followed in some cases by incubation with biotinylated anti-CD45.1 or anti-Thy1.1 antibody and positive selection with anti-biotin microbeads (Miltenyi Biotec). For cytokine response assays, purified CD8+ cells (2 × 10^5 total) were cultured in the presence of irradiated syngeneic cells with or without common γ chain family cytokines IL-2 (10 U/ml; Roche), IL-7 (5 ng/ml; R&D Systems), or IL-15 (5 ng/ml; R&D Systems).

Antibodies, tetramers, and flow cytometry. The following antibodies were used for cell surface staining: anti-CD4–FITC, –PE or –APC (L3T4), anti-CD8α–PE or –APC (Ly-2), anti-CD45.1–FITC, –APC, or –biotin (A20), anti-B220–PE-Cy5 (RA3-6B2), anti-CD11b–APC (M1/70), anti-D^d–biotin (34-2-12), anti-CD44–FITC, –APC, or –Alexa Fluor 750 (IM7), anti-CD62L–PE or –FITC (MEL-14), anti-CD127–PE (SB/199), and anti-Thy1.1–FITC or –biotin (HIS 51) purchased from eBioscience; anti-CD45.2–PerCP (104), anti–PD-1–PE (J43), and anti-Vβ8.3 TCR (1B3.3) purchased from BD Biosciences. Detection of biotinylated antibodies was performed using FITC, PerCP, or APC conjugated to streptavidin (BD Biosciences). Detection of CD8+ T cells bearing the 2C TCR was carried out using the clonotype-specific mAb 1B2, and anti-mouse IgG1–APC (X56; BD Biosciences). Detection of H60-specific cells was performed by K^b/LTFNYRNL pentamer (ProImmune). Intracellular staining was carried out using anti–IFN-γ–APC (XMG1.2; BD Biosciences), anti-Foxp3–APC (FJK-16s; eBioscience) and the appropriate isotype controls. Intranuclear staining for BrdU was carried out using anti-BrdU–APC flow kit (BD Biosciences) according to the manufacturer's instructions.

Cell-mediated lymphocytotoxicity assay. Cell-mediated lymphocytotoxicity (CML) assays were preformed as previously described (75).

IFN-γ responses. Responder cells were resuspended in CML medium (75) and mixed with irradiated stimulator cells as in the CML assay. Cells were cultured for 20 hours, and Brefeldin A was added at 10 μg/ml for the final 4 hours. IFN-γ was detected as above with cells costained for CD8, congenic markers, or Vβ8.3. In some experiments, anti–PD-L1 or isotype control was added at 5 μg/ml from the start of culture. H60 (LTFNYRNL), UTY (WMHHNMDLI), and irrelevant (OVA SIINFEKL) peptides (ProImmune) were used in some assays at a concentration of 1 μg/ml (UTY) or 20 ng/ml (H60).

Ex vivo CFSE proliferation assay. Responder SCs were labeled with 2 μM CFSE, washed, and plated with irradiated syngeneic (B6) or allogeneic (BDF1) SCs at a 1:1 ratio as in the CML assay. After 5 days, CFSE dilution was assessed by flow cytometry on cells costained for CD4, CD8, and congenic markers and using dead cell exclusion by propidium iodide staining (BD Biosciences). In some experiments, anti–PD-L1 or isotype control was added at 5 μg/ml from the start of culture.

In vivo cytotoxicity assay. Specific in vivo cytotoxicity of host B cells was determined as described previously (15).

Histological scoring. Histopathologic analysis of GVHD target organs was performed single blind, as reported previously (3), by scoring changes in skin (dermal/epidermal lymphocyte infiltration, dyskeratotic epidermal keratinocytes, epidermal thickening), liver (portal tract inflammatory infiltration, lymphocytic infiltration of bile ducts, bile duct epithelial apoptosis, vascular endothelialitis, parenchymal apoptosis, parenchymal microabscesses, parenchymal mitotic figures), and colon (crypt regeneration, apoptosis in crypt epithelial cells, crypt loss, surface colonocyte attenuation, inflammatory cell infiltration in lamina propria, mucosal

ulceration, thickening of mucosa). A severity scale from 0 to 4 was used: 0, normal; 0.5, focal and rare; 1, focal and mild; 2, diffuse and mild; 3, diffuse and moderate; 4, diffuse and severe.

Statistics. Statistical analyses were performed using the Mann-Whitney test or the Wilcoxon test in the case of paired data. A *P* value less than 0.05 was considered significant.

1. Kolb HJ, Schmid C, Barrett AJ, Schendel DJ. Graft-versus-leukemia reactions in allogeneic chimeras. *Blood*. 2004;103(3):767–776.
2. Sprangers B, Van Wijmeersch B, Fevery S, Waer M, Billiau AD. Experimental and clinical approaches for optimization of the graft-versus-leukemia effect. *Nat Clin Pract Oncol*. 2007;4(7):404–414.
3. Chakraverty R, et al. An inflammatory checkpoint regulates recruitment of graft-versus-host reactive T cells to peripheral tissues. *J Exp Med*. 2006; 203(8):2021–2031.
4. Hill GR, Crawford JM, Cooke KR, Brinson YS, Pan L, Ferrara JL. Total body irradiation and acute graft-versus-host disease: the role of gastrointestinal damage and inflammatory cytokines. *Blood*. 1997;90(8):3204–3213.
5. Xun CQ, Thompson JS, Jennings CD, Brown SA, Widmer MB. Effect of total body irradiation, busulfan-cyclophosphamide, or cyclophosphamide conditioning on inflammatory cytokine release and development of acute and chronic graft-versus-host disease in H-2-incompatible transplanted SCID mice. *Blood*. 1994;83(8):2360–2367.
6. Zhang Y, Joe G, Hexner E, Zhu J, Emerson SG. Host-reactive CD8(+) memory stem cells in graft-versus-host disease. *Nat Med*. 2005;11(12):1299–1305.
7. Billiau AD, Fevery S, Rutgeerts O, Landuyt W, Waer M. Crucial role of timing of donor lymphocyte infusion in generating dissociated graft-versus-host and graft-versus-leukemia responses in mice receiving allogeneic bone marrow transplants. *Blood*. 2002;100(5):1894–1902.
8. Johnson BD, Truitt RL. Delayed infusion of immunocompetent donor cells after bone marrow transplantation breaks graft-host tolerance allows for persistent antileukemic reactivity without severe graft-versus-host disease. *Blood*. 1995;85(11):3302–3312.
9. Sykes M, Bukhari Z, Sachs DH. Graft-versus-leukemia effect using mixed allogeneic bone marrow transplantation. *Bone Marrow Transplant*. 1989;4(5):465–474.
10. Peggs KS, et al. Dose-escalated donor lymphocyte infusions following reduced intensity transplantation: toxicity, chimerism, and disease responses. *Blood*. 2004;103(4):1548–1556.
11. Chakraverty R, et al. Host MHC class II+ antigen-presenting cells and CD4 cells are required for CD8-mediated graft-versus-leukemia responses following delayed donor leukocyte infusions. *Blood*. 2006;108(6):2106–2113.
12. Ghosh A, et al. Donor T cells primed on leukemia lysate-pulsed recipient APCs mediate strong graft-versus-leukemia effects across MHC barriers in full chimeras. *Blood*. 2009;113(18):4440–4448.
13. Mapara MY, Kim YM, Wang SP, Bronson R, Sachs DH, Sykes M. Donor lymphocyte infusions mediate superior graft-versus-leukemia effects in mixed compared to fully allogeneic chimeras: a critical role for host antigen-presenting cells. *Blood*. 2002; 100(5):1903–1909.
14. Xia G, Truitt RL, Johnson BD. Graft-versus-leukemia and graft-versus-host reactions after donor lymphocyte infusion are initiated by host-type antigen-presenting cells and regulated by regulatory T cells in early and long-term chimeras. *Biol Blood Marrow Transplant*. 2006;12(4):397–407.
15. Chakraverty R, et al. The host environment regulates the function of CD8+ graft-versus-host-reactive effector cells. *J Immunol*. 2008;181(10):6820–6828.
16. Durakovic N, et al. Factors governing the activation of adoptively transferred donor T-cells infused after allogeneic bone marrow transplantation in the mouse. *Blood*. 2007;109(10):4564–4574.
17. Mapara MY, Kim YM, Marx J, Sykes M. Donor lymphocyte infusion-mediated graft-versus-leukemia effects in mixed chimeras established with a nonmyeloablative conditioning regimen: extinction of graft-versus-leukemia effects after conversion to full donor chimerism. *Transplantation*. 2003;76(2):297–305.
18. Meunier MC, Baron C, Perreault C. Two host factors regulate persistence of H7-specific T cells injected in tumor-bearing mice. *PLoS One*. 2009;4(1):e4116.
19. Boon T, Coulie PG, Van den Eynde BJ, van der Bruggen P. Human T cell responses against melanoma. *Annu Rev Immunol*. 2006;24:175–208.
20. Shin H, Wherry EJ. CD8 T cell dysfunction during chronic viral infection. *Curr Opin Immunol*. 2007;19(4):408–415.
21. Wherry EJ, Blattman JN, Murali-Krishna K, van der Most R, Ahmed R. Viral persistence alters CD8 T-cell immunodominance and tissue distribution and results in distinct stages of functional impairment. *J Virol*. 2003;77(8):4911–4927.
22. Barber DL, et al. Restoring function in exhausted CD8 T cells during chronic viral infection. *Nature*. 2006;439(7077):682–687.
23. van Rhee F, et al. Adoptive immunotherapy for relapse of chronic myeloid leukemia after allogeneic bone marrow transplant: equal efficacy of lymphocytes from sibling and matched unrelated donors. *Bone Marrow Transplant*. 1998;21(10):1055–1061.
24. Yamamoto R, et al. PD-1-PD-1 ligand interaction contributes to immunosuppressive microenvironment of Hodgkin lymphoma. *Blood*. 2008; 111(6):3220–3224.
25. Kaech SM, Wherry EJ. Heterogeneity and cell-fate decisions in effector and memory CD8+ T cell differentiation during viral infection. *Immunity*. 2007;27(3):393–405.
26. Bannard O, Kraman M, Fearon DT. Secondary replicative function of CD8+ T cells that had developed an effector phenotype. *Science*. 2009; 323(5913):505–509.
27. Joshi NS, et al. Inflammation directs memory precursor and short-lived effector CD8(+) T cell fates via the graded expression of T-bet transcription factor. *Immunity*. 2007;27(2):281–295.
28. Sarkar S, Kalia V, Haining WN, Konieczny BT, Subramaniam S, Ahmed R. Functional and genomic profiling of effector CD8 T cell subsets with distinct memory fates. *J Exp Med*. 2008;205(3):625–640.
29. Mueller SN, Ahmed R. High antigen levels are the cause of T cell exhaustion during chronic viral infection. *Proc Natl Acad Sci U S A*. 2009; 106(21):8623–8628.
30. Golden-Mason L, Palmer B, Klarquist J, Mengshol JA, Castelblanco N, Rosen HR. Upregulation of PD-1 expression on circulating and intrahepatic hepatitis C virus-specific CD8+ T cells associated with reversible immune dysfunction. *J Virol*. 2007; 81(17):9249–9258.
31. Katou F, Ohtani H, Watanabe Y, Nakayama T, Yoshie O, Hashimoto K. Differing phenotypes between intraepithelial and stromal lymphocytes in early-stage tongue cancer. *Cancer Res*. 2007;67(23):11195–11201.
32. Keir ME, et al. Tissue expression of PD-L1 mediates peripheral T cell tolerance. *J Exp Med*. 2006; 203(4):883–895.
33. Heath WR, Carbone FR. Cross-presentation, dendritic cells, tolerance and immunity. *Annu Rev Immunol*. 2001;19:47–64.
34. Kean LS, et al. NK cells mediate costimulation blockade-resistant rejection of allogeneic stem cells during nonmyeloablative transplantation. *Am J Transplant*. 2006;6(2):292–304.
35. Sallusto F, Geginat J, Lanzavecchia A. Central memory and effector memory T cell subsets: function, generation, and maintenance. *Annu Rev Immunol*. 2004;22:745–763.
36. Sha WC, Nelson CA, Newberry RD, Kranz DM, Russell JH, Loh DY. Positive and negative selection of an antigen receptor on T cells in transgenic mice. *Nature*. 1988;336(6194):73–76.
37. Speir JA, et al. Structural basis of 2C TCR allorecognition of H-2Ld peptide complexes. *Immunity*. 1998; 8(5):553–562.
38. Billiau AD, Fevery S, Rutgeerts O, Landuyt W, Waer M. Transient expansion of Mac1+Ly6-G+ Ly6-C+ early myeloid cells with suppressor activity in spleens of murine radiation marrow chimeras: possible implications for the graft-versus-host and graft-versus-leukemia reactivity of donor lymphocyte infusions. *Blood*. 2003;102(2):740–748.
39. Krause DS, Van Etten RA. Adoptive immunotherapy of BCR-ABL-induced chronic myeloid leukemia-like myeloproliferative disease in a murine model. *Blood*. 2004;104(13):4236–4244.
40. Valujskikh A, Lantz O, Celli S, Matzinger P, Heeger PS. Cross-primed CD8(+) T cells mediate graft rejection via a distinct effector pathway. *Nat Immunol*. 2002;3(9):844–851.
41. Blackburn SD, Shin H, Freeman GJ, Wherry EJ. Selective expansion of a subset of exhausted CD8 T cells by alphaPD-L1 blockade. *Proc Natl Acad Sci U S A*. 2008;105(39):15016–15021.
42. Blazar BR, et al. Host T cells resist graft-versus-host disease mediated by donor leukocyte infusions. *J Immunol*. 2000;165(9):4901–4909.
43. Laouar A, Manocha M, Haridas V, Manjunath N. Concurrent generation of effector and central memory CD8 T cells during vaccinia virus infection. *PLoS One*. 2008;3(12):e4089.
44. Obar JJ, Lefrancois L. Early signals during CD8(+) T cell priming regulate the generation of central

memory cells. *J Immunol*. 2010;185(1):263–272.

45. Li Q, et al. Visualizing antigen-specific and infected cells in situ predicts outcomes in early viral infection. *Science*. 2009;323(5922):1726–1729.

46. Rocha B, Grandien A, Freitas AA. Anergy and exhaustion are independent mechanisms of peripheral T cell tolerance. *J Exp Med*. 1995;181(3):993–1003.

47. Scholer A, Hugues S, Boissonnas A, Fetler L, Amigorena S. Intercellular adhesion molecule-1-dependent stable interactions between T cells and dendritic cells determine CD8+ T cell memory. *Immunity*. 2008;28(2):258–270.

48. Marzo AL, Klonowski KD, Le Bon A, Borrow P, Tough DF, Lefrancois L. Initial T cell frequency dictates memory CD8+ T cell lineage commitment. *Nat Immunol*. 2005;6(8):793–799.

49. Teixeiro E, et al. Different T cell receptor signals determine CD8+ memory versus effector development. *Science*. 2009;323(5913):502–505.

50. Rutishauser RL, et al. Transcriptional repressor Blimp-1 promotes CD8(+) T cell terminal differentiation and represses the acquisition of central memory T cell properties. *Immunity*. 2009;31(2):296–308.

51. Gattinoni L, et al. Wnt signaling arrests effector T cell differentiation and generates CD8+ memory stem cells. *Nat Med*. 2009;15(7):808–813.

52. Araki K, et al. mTOR regulates memory CD8 T-cell differentiation. *Nature*. 2009;460(7251):108–112.

53. Redmond WL, Sherman LA. Peripheral tolerance of CD8 T lymphocytes. *Immunity*. 2005;22(3):275–284.

54. Wherry EJ, et al. Molecular signature of CD8+ T cell exhaustion during chronic viral infection. *Immunity*. 2007;27(4):670–684.

55. Kawase T, et al. HLA mismatch combinations associated with decreased risk of relapse: implications for the molecular mechanism. *Blood*. 2009;113(12):2851–2858.

56. Rutten CE, et al. HLA-DP as specific target for cellular immunotherapy in HLA class II-expressing B-cell leukemia. *Leukemia*. 2008;22(7):1387–1394.

57. Dodero A, et al. Haploidentical stem cell transplantation after a reduced-intensity conditioning regimen for the treatment of advanced hematologic malignancies: posttransplantation CD8-depleted donor lymphocyte infusions contribute to improve T-cell recovery. *Blood*. 2009;113(19):4771–4779.

58. Ferber I, Schonrich G, Schenkel J, Mellor AL, Hammerling GJ, Arnold B. Levels of peripheral T cell tolerance induced by different doses of tolerogen. *Science*. 1994;263(5147):674–676.

59. Kloosterboer FM, et al. Direct cloning of leukemia-reactive T cells from patients treated with donor lymphocyte infusion shows a relative dominance of hematopoiesis-restricted minor histocompatibility antigen HA-1 and HA-2 specific T cells. *Leukemia*. 2004;18(4):798–808.

60. Malarkannan S, et al. The molecular and functional characterization of a dominant minor H antigen, H60. *J Immunol*. 1998;161(7):3501–3509.

61. Beatty GL, et al. Functional unresponsiveness and replicative senescence of myeloid leukemia antigen-specific CD8+ T cells after allogeneic stem cell transplantation. *Clin Cancer Res*. 2009;15(15):4944–4953.

62. Zhang Y, Joe G, Hexner E, Zhu J, Emerson SG. Alloreactive memory T cells are responsible for the persistence of graft-versus-host disease. *J Immunol*. 2005;174(5):3051–3058.

63. Blaser BW, et al. Trans-presentation of donor-derived interleukin 15 is necessary for the rapid onset of acute graft-versus-host disease but not for graft-versus-tumor activity. *Blood*. 2006;108(7):2463–2469.

64. Kosaka H, Sprent J. Tolerance of CD8+ T cells developing in parent-->F1 chimeras prepared with supralethal irradiation: step-wise induction of tolerance in the intrathymic and extrathymic environments. *J Exp Med*. 1993;177(2):367–378.

65. Lee JW, et al. Peripheral antigen display by lymph node stroma promotes T cell tolerance to intestinal self. *Nat Immunol*. 2007;8(2):181–190.

66. Mueller SN, Ahmed R. Lymphoid stroma in the initiation and control of immune responses. *Immunol Rev*. 2008;224:284–294.

67. Davenport MP, Belz GT, Ribeiro RM. The race between infection and immunity: how do pathogens set the pace? *Trends Immunol*. 2009;30(2):61–66.

68. Mueller SN, et al. Viral targeting of fibroblastic reticular cells contributes to immunosuppression and persistence during chronic infection. *Proc Natl Acad Sci U S A*. 2007;104(39):15430–15435.

69. Asakura S, et al. Alloantigen expression on nonhematopoietic cells reduces graft-versus-leukemia effects in mice. *J Clin Invest*. 2010;120(7):2370–2378.

70. Mueller SN, et al. PD-L1 has distinct functions in hematopoietic and nonhematopoietic cells in regulating T cell responses during chronic infection in mice. *J Clin Invest*. 2010;120(7):2508–2515.

71. Shlomchik WD, et al. Prevention of graft versus host disease by inactivation of host antigen-presenting cells. *Science*. 1999;285(5426):412–415.

72. Teshima T, et al. Acute graft-versus-host disease does not require alloantigen expression on host epithelium. *Nat Med*. 2002;8(6):575–581.

73. Rodig N, et al. Endothelial expression of PD-L1 and PD-L2 down-regulates CD8+ T cell activation and cytolysis. *Eur J Immunol*. 2003;33(11):3117–3126.

74. Zang W, et al. Inhibition of the alloimmune response through the generation of regulatory T cells by a MHC class II-derived peptide. *J Immunol*. 2008; 181(11):7499–7506.

75. Sykes M, Szot GL, Swenson KA, Pearson DA. Induction of high levels of allogeneic hematopoietic reconstitution and donor-specific tolerance without myelosuppressive conditioning. *Nat Med*. 1997; 3(7):783–787.